

Melting Behavior of Polypropylene Fibers Studied by Differential Scanning Calorimetry

ERIK ANDREASSEN,^{1,*} KRISTIN GRØSTAD,² OLE JAN MYHRE,² MARIANNE D. BRAATHEN,²
EINAR L. HINRICHSEN,¹ ANNE MARIE V. SYRE,² and TOR BERTEL LØVGREN²

¹Sintef, P.O. Box 124 Blindern, N-0314 Oslo, Norway; ²Borealis AS, N-3960 Stathelle, Norway

SYNOPSIS

Polypropylene fibers produced in a compact-spinning process were studied by differential scanning calorimetry (DSC). With unrestrained fibers, the onset of melting increases with decreasing draw ratio, increasing M_w/M_n , decreasing extrusion temperature, increasing annealing ratio, and increasing draw-down ratio. These trends are discussed in terms of restraints and reorganization. The onset of melting is shifted to lower temperatures as the heating rate increases for all combinations of material and processing parameters, indicating suppressed reorganization. At low draw ratios, the height and width of the endotherm are affected by the spinline stress, and a secondary peak or shoulder is observed on the high temperature side of the main peak. The magnitude of the secondary peak increases with decreasing M_w/M_n , increasing draw ratio, decreasing draw-down ratio, and decreasing heating rate, but its position mainly depends on the heating rate. This indicates that the secondary peak may be due to the melting of structures that have been reorganized during the heating scan. As the draw ratio increases, the melting regime broadens, especially towards lower temperatures, and several maxima emerge on the DSC curve. Reorganization and shrinkage during heating may explain these observations. © 1995 John Wiley & Sons, Inc.

INTRODUCTION

A DSC heating scan provides a fingerprint of the sample, containing information about the processing history and material parameters. Using statistical methods, a set of DSC curves can be "calibrated" to yield structural information otherwise only directly available by techniques such as wide-angle x-ray scattering (WAXS). Furthermore, the melting dynamics observed by DSC provides supplementary information about structural restraints and molecular mobility. DSC analyses also have more direct applications, e.g., in assessing the bondability of fibers to be used in thermobonded nonwoven fabrics.

DSC thermograms obtained for oriented polymers are generally not well understood. Endotherms with several maxima are often observed for oriented polymers. Different interpretations can be found in the literature. One of the debated issues is to what extent

structural reorganization during heating influence the thermograms. The position and the shape of the endotherm depend on the processing and material parameters of the polymer sample, the sample preparation technique, and the heating rate. There are variations in published data for seemingly similar samples, but DSC curves are reproducible for a given instrument and sample preparation technique.

This article deals with polypropylene (PP) fibers produced in a compact-spinning process. The structure development in this process and the tensile properties of the fibers have been discussed earlier.¹⁻³ Effects of processing parameters and molecular weight distribution (MWD) on the DSC thermograms will be presented in this article. The results will be discussed in terms of structure, structural restraints, and reorganization.

EXPERIMENTAL

The fibers were produced in two different full-scale compact-spinning lines. The compact-spinning

* To whom correspondence should be addressed.

process consists of three integrated stages: (melt) spinning, (solid state) drawing, and annealing. The parameters of this process are the temperatures and the deformation ratios of these three stages. The draw-down ratio is defined as the ratio of spinning speed to extrusion speed. The draw ratio is defined as the ratio of output speed to input speed for the drawing stage (the latter being equal to the spinning speed). Finally, the annealing ratio is defined as the difference between input speed and output speed for the annealing stage, divided by input speed. (The output speed of the annealing stage is the same as the line speed in Table I.) The annealing ratio is positive, i.e., the fibers are allowed to shrink in the annealing stage. Further details of the compact-spinning process are given in refs. 2 and 4. The main processing parameters that were varied in this study are listed in Table I.

The materials are highly isotactic homopolymers. Material parameters, i.e., M_w and M_w/M_n , have been varied independently (see Table I). Grades with narrow MWDs were obtained by peroxide degradation. Hence, for the grades referred to below, having equal M_w but different M_w/M_n , the high molecular weight tail has been "removed" for the narrow MWD grade.

The results reported in this article are based on a total of about 100 different PP fibers. The span in MWD and processing parameters was made as large as possible—the limiting factor being the stability of the process—and it should cover most of the relevant industrial processing conditions. Reduced factorial designs were employed for the variation of molecular weight characteristics and processing parameters. The trends in the DSC data were analyzed by statistical methods.

The DSC measurements were performed with a Perkin-Elmer DSC-7 instrument. Different sample preparation techniques were considered.^{5,6} An important criterion was that the chosen technique should be suitable for industrial routine measurements. Hence, the simplest method that gave reproducible results, while showing significant differences between samples with different material and processing parameters, was selected. With this method, fibers were cut into 4 mm long segments, which were aligned parallel in the aluminium pan. The sample weights were around 2 mg. The pan was then sealed with the Perkin-Elmer standard crimper press. The pressure that was applied was sufficient for good thermal contact between pan and fibers, but the DSC thermograms indicate that the fibers were relatively unrestrained. Except when otherwise

Table I Material and Processing Parameters,^a with Associated Ranges, as Examined in this Study

Parameter	Range
M_w ^b	160000–230000
M_w/M_n	3.4–5.8
# orifices in the spinneret	9000–30500
Die diameter	0.25–0.4 mm
Draw-down ratio	24–360
Extrusion temperature	220–280°C
Draw ratio	1.2–3.5
Drawing temperature	20–180°C
Annealing ratio	0.02–0.07
Annealing temperature	150–180°C
Line speed	40–130 m/min
Linear density ^c of fibers	2–11 dtex

^a See main text and ref. 2 for definitions and further details.

^b The melt flow indices were in the range 8–25.

^c The linear density is measured in tex: 1 tex = 1 g/km. The diameter can be calculated from the linear density using the bulk density.

stated, the heating rate was 10 K/min. Indium was used as a calibration standard.

RESULTS

Fibers with Low Draw Ratios

When the draw ratio imposed in the drawing stage is low (≤ 2), the thermograms typically consist of one major endotherm and a small secondary peak or shoulder at a higher temperature. The draw ratio is the dominant processing parameter. Hence, effects of spinning parameters are generally more clearly seen when the draw ratio is low. The onset of melting and the peak of the major endotherm are generally correlated. Hence, the trends reported for the onset values are also observed for the peak values, and vice versa.

The structure development in the spinning stage is affected by the spinline stress and the high molecular weight tail of the MWD (i.e., M_w/M_n , cf. the Experimental section). This topic was discussed in an earlier publication.² However, some of the relations that will be referred to below are summarized in the remainder of this paragraph. The spinline stress increases with increasing draw-down ratio, decreasing extrusion temperature, and increasing M_w . The structure of fibers with low draw ratios, which is dominated by spinning stage effects, is either the mesomorphic form with uniaxial orientation or the crystalline α phase with bimodal orientation.

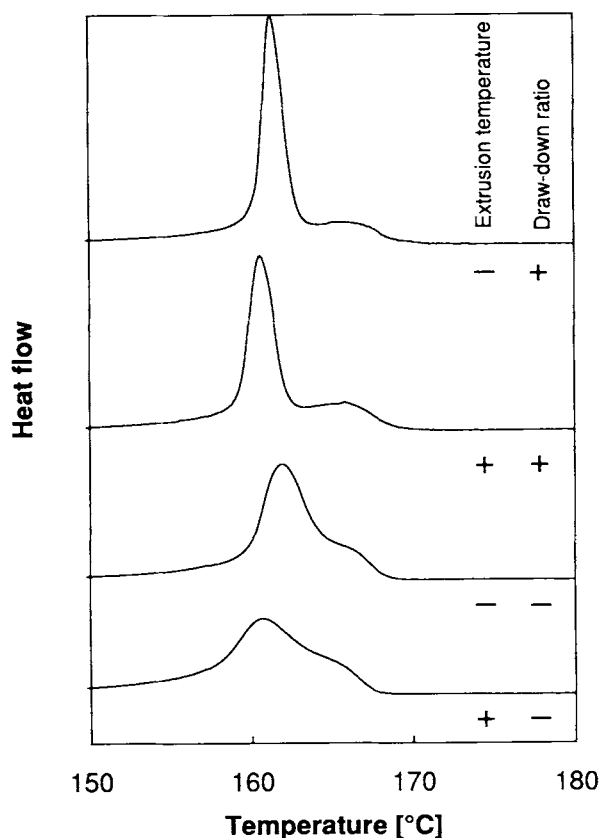


Figure 1 Effects of spinning parameters on the thermograms. The extrusion temperature and the draw-down ratio are varied in two levels (-/+); 220°C/280°C and 57/156, respectively. The draw ratio is low (1.5) for these fibers, and a standard commercial material with melt flow index = 14 and $M_w/M_n = 5.5$ is used.

High spinline stresses and broad MWDs lead to the latter type of structure. Nucleation, in which the longest chains form row nuclei, is a local process, and, hence, not directly related to the stress in a continuum-mechanical sense. The degree of orientation of structural elements increases with increasing spinline stress for both types of structure.

The height and the width of the endotherms are affected by the spinline stress, as shown in Figure 1. As can be seen, changing the draw-down ratio has a larger effect on the endotherm than changing the extrusion temperature. The same trend was observed for other properties related to the spinline stress, such as the degree of molecular orientation and the tensile strength. (The low and high levels of the extrusion temperature in Fig. 1 are close to the extreme values for this process, while those of the draw-down ratio are well inside the processing window, cf. Table I.) The heat of fusion (the integral

of the endotherm) increases with increasing spinline stress.

The position of the endothermic peak is negatively correlated with the extrusion temperature. The effect is small, but significant (cf. Fig. 1). When the draw-down ratios are low, as in Figure 1, the peak position is almost uncorrelated with the draw-down ratio. At high draw-down ratios (≥ 200), the peak shifts to higher temperatures with increasing draw-down ratio.

The peak position is also related to material parameters. It shifts to higher temperatures with increasing M_w/M_n (Fig. 2), but it is independent of M_w for the rather limited M_w interval covered in this study. Both fibers in Figure 2 have α -crystalline structure with bimodal orientation, due to the high draw-down ratio. At lower draw-down ratios, the structure of the narrow MWD fiber is mesomorphic, and the peak positions of broad and narrow MWD fibers differ more than in Figure 2.

A shoulder or secondary peak appears on the high temperature side of the main peak for certain pa-

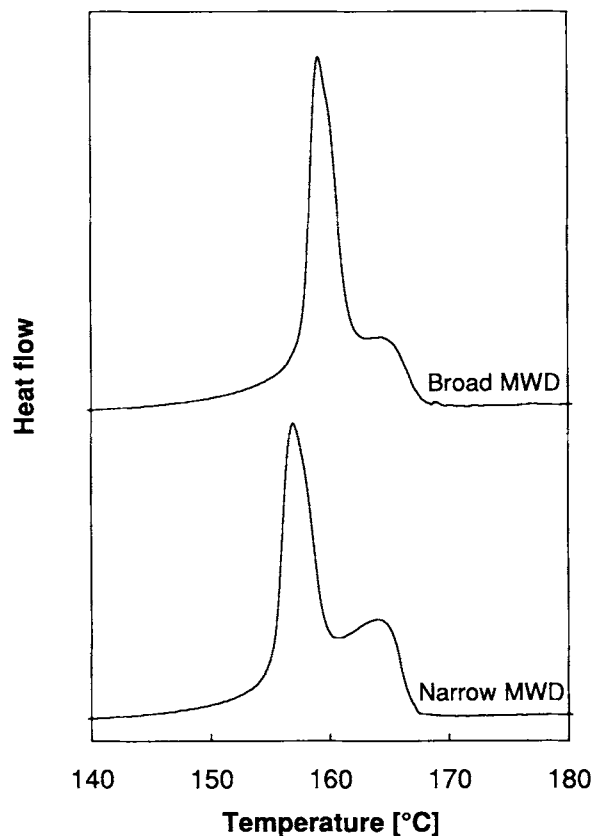


Figure 2 Effects of M_w/M_n on the thermograms. M_w/M_n is 4.7 and 3.8 for the broad and the narrow MWD, respectively. The melt flow index is 16, the draw-down ratio is 151, and the draw ratio is 1.6, for both fibers.

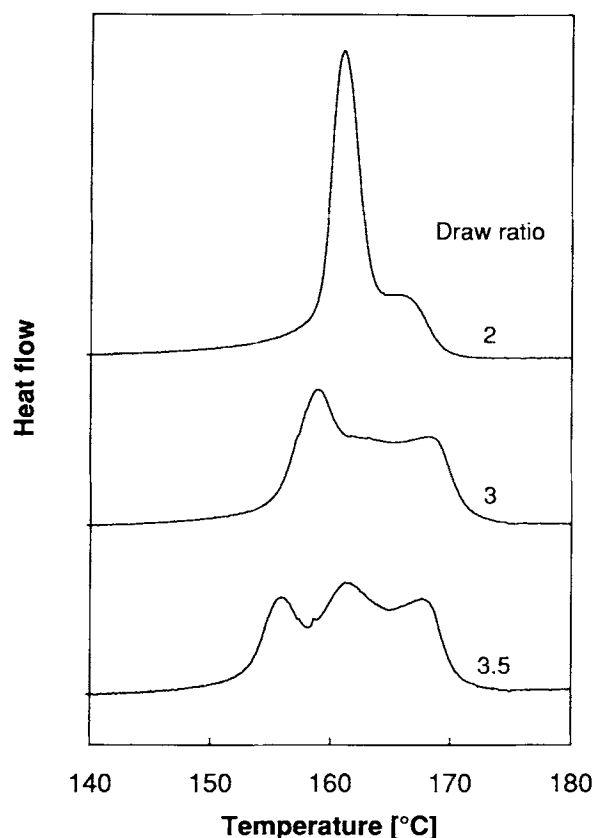


Figure 3 Effects of draw ratio on the thermograms. The material is the same as in Figure 1.

rameters. This peak increases, relative to the main peak, with increasing draw ratio, decreasing draw-down ratio, and decreasing M_w/M_n (Fig. 2).

The temperature at which the last structural element melts is positively correlated to the spinline stress (Fig. 1). These shifts are smaller than those of the onset of melting and the major peak reported above.

Fibers with High Draw Ratios

As for other fiber properties, the draw ratio is the single most important parameter for the thermal properties studied by DSC (cf. Fig. 3). The melting regime broadens with increasing draw ratio—the onset of melting shifts to lower temperatures, and the (upper) end of the melting regime shifts to higher temperatures. A decrease in drawing temperature corresponds to an increase in the effective draw ratio, since the deformation will be more effective.² However, the sensitivity to drawing temperatures in the range specified in Table I is low.

The extrusion temperature and the spinline stress affect the onset of melting and the end of the melting

regime, respectively, as described for fibers with low draw ratios. (The spinline stress is a function of the extrusion temperature and the draw-down ratio, as mentioned above.) In fact, these effects are more pronounced when the draw ratio is high (cf. Fig. 4). The onset of melting also increases with increasing M_w/M_n , as for fibers with low draw ratios.

At high draw ratios (≥ 3.5), the DSC curves typically have three maxima. The first of these peaks seems to correspond to the main peak observed for fibers with low draw ratios. The height of this first peak increases with decreasing extrusion temperature, as shown in Figure 4. The heat of fusion increases with increasing draw ratio.

Effects of annealing stage parameters have only been studied for fibers with high draw ratios. As for the tensile properties,² the annealing ratio has a stronger influence than the annealing temperature. When the annealing ratio is increased from 0.02 to 0.07, for a typical annealing temperature of 150°C, the onset of melting increases by 1–2°C. The end of the melting regime is not influenced by the annealing ratio.

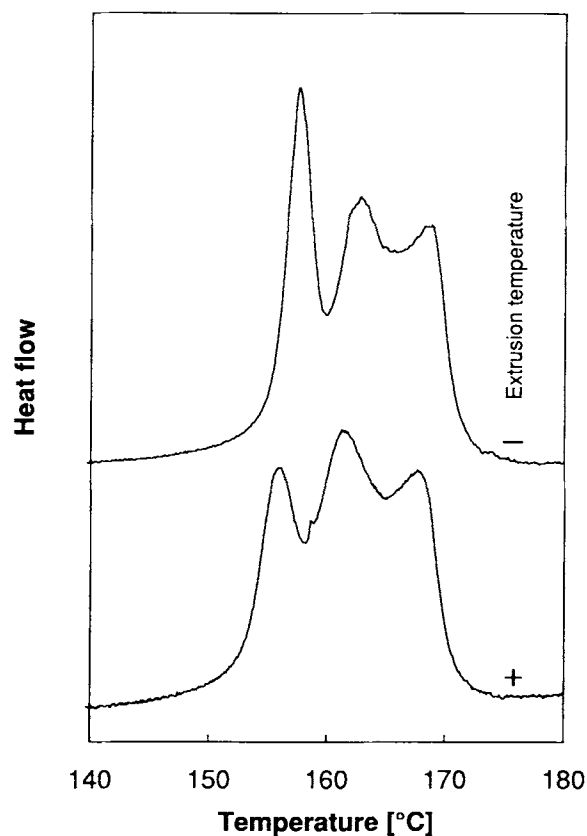


Figure 4 Effects of extrusion temperature (–/+ corresponds to 220°C/280°C) for fibers with a high draw ratio (3.5). The material is the same as in Figure 1.

Effects of Heating Rate

The onset of melting shifts to lower temperatures as the heating rate increases for all combinations of material and processing parameters, while the end of the melting regime remains at almost the same temperature. The secondary peak is shifted to lower temperatures and decreases in magnitude as the heating rate increases. The shifts of the secondary peak are comparable to those of the major peak (in some cases slightly larger).

As shown in Figure 5, the onset of melting decreases logarithmically on the interval considered in this study, i.e.,

$$T_{\text{onset}} = A - B \log \dot{T}. \quad (1)$$

For the standard commercial grade in Figure 5, the difference in onset of melting between fibers with low and high draw ratios is independent of the heating rate. However, generally, the slope [B in eq. (1)] varies somewhat with material and processing parameters. Specifically, the difference between the onset of melting for a fiber with high draw ratio and broad MWD, and that for a fiber with low draw ratio and narrow MWD seems to decrease with increasing heating rate (Fig. 6). At all heating rates in this study, fibers with high draw ratios and narrow MWDs have the lowest onset of melting values, while fibers with low draw ratios and broad MWDs

have the highest values, as indicated by the solid and dotted lines in Figure 6.

The recorded heat of fusion also decreases with increasing heating rate (Fig. 7). At high heating rates, the differences between fibers are small. If the fibers in Figure 7 are recrystallized after melting (cooling rate 10 K/min), the (negative) heats of fusion of this process are close to the (positive) values at the highest heating rate in Figure 7.

The onset of melting for the unprocessed material (pellets) decreases linearly with increasing heating rate (Fig. 8), while the heat of fusion is almost constant.

DISCUSSION

Restrained vs. Unrestrained Samples

In most DSC analyses, the melting does not occur at equilibrium. The key words here are metastability, reorganization, and superheating. A metastable structure will reorganize towards a more stable one during heating. Defects will be healed and crystallite dimensions will increase. The degree of reorganization and the melting point decrease, and the information about the original sample increases with increasing heating rate. However, superheating occurs at high heating rates if the melting kinetics is too slow relative to the heating rate. Superheating

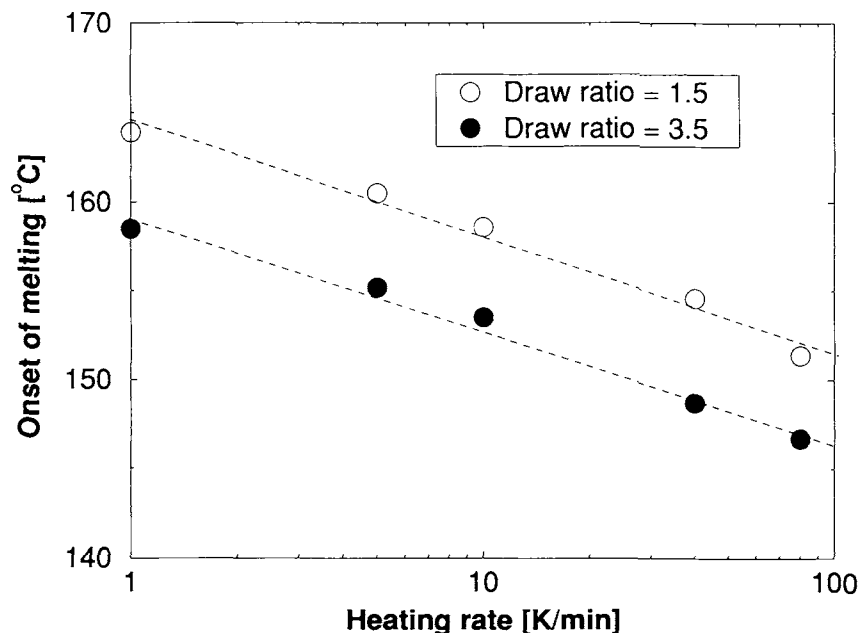


Figure 5 Onset of melting vs. heating rate for fibers with low and high draw ratios. The material is the same as in Figure 1.

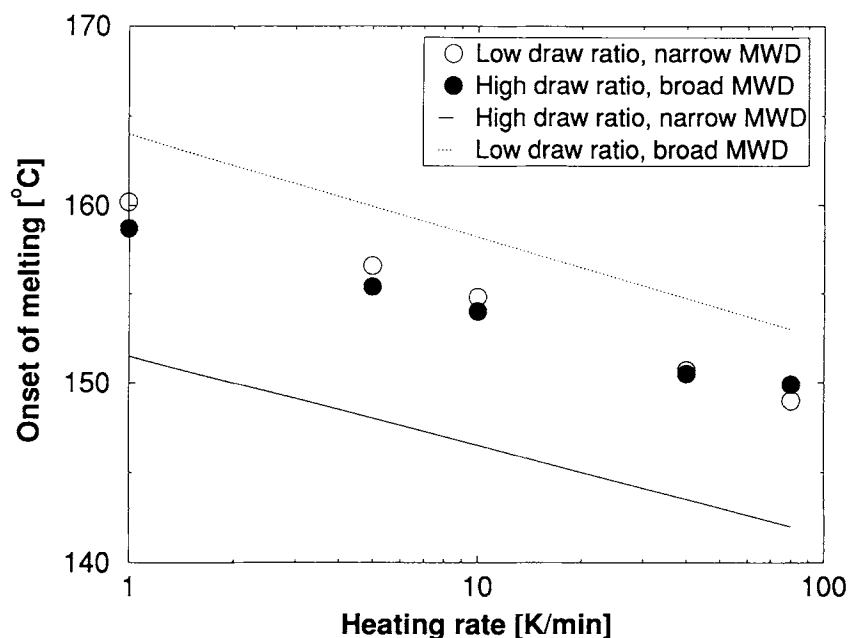


Figure 6 Onset of melting vs. heating rate for fibers with different M_w/M_n (3.0 and 4.7) and draw ratio (1.5 and 3.0). The melt flow index is 8 for both fibers. Upper and lower limits for our data set are indicated by dotted and solid lines (see main text for details).

shifts the endotherm to higher temperatures. (The onset of melting is not affected by true superheating, i.e., when the melting kinetics of the constituent crystallites, not taking into account internal and external restraints, is too slow.)⁷ Also, at high heating rates, the temperature field will be less homo-

geneous inside the sample. Hence, the thermograms may be affected by the sample size.

Oriented polymer samples are prone to reorganization and superheating. The restraints of the sample during heating play an important role. For samples of drawn poly(ethylene terephthalate)

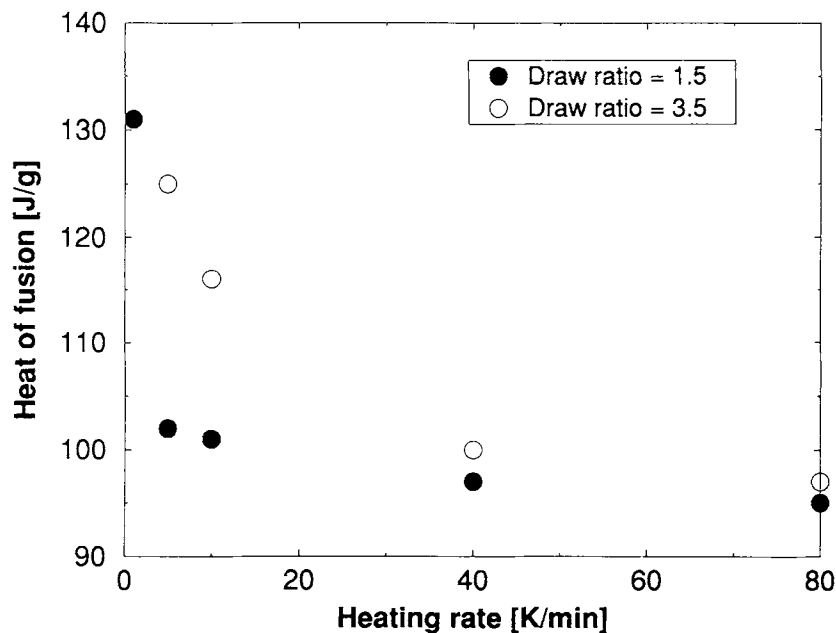


Figure 7 Heat of fusion vs. heating rate for fibers with low and high draw ratios. The fibers are the same as in Figure 5.

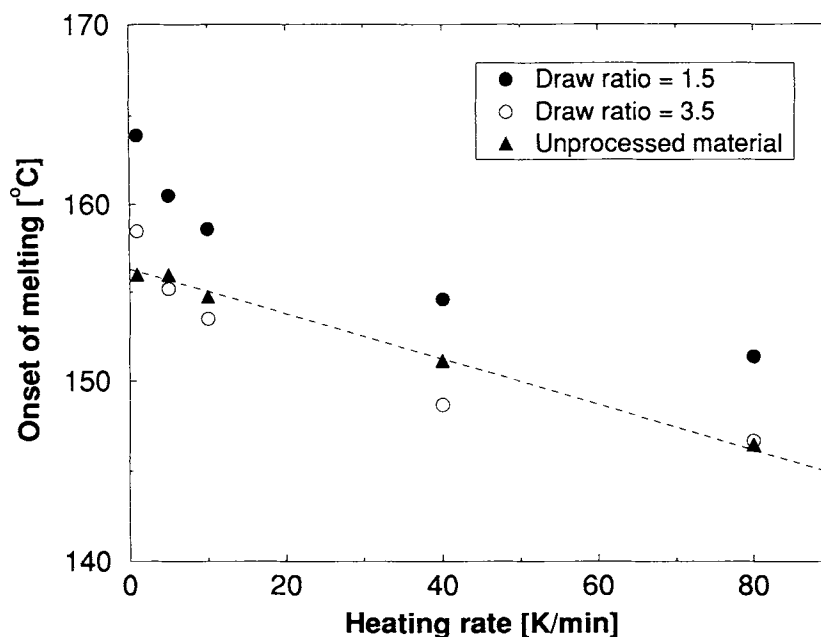


Figure 8 Onset of melting vs. heating rate for the unprocessed material. The data for the two fibers are the same as in Figure 5.

(PET), Wunderlich⁷ observed that the melting temperature decreased with increasing heating rate (interpreted as suppressed reorganization) when the sample was unrestrained, while the opposite (interpreted as superheating) was observed when the sample was restrained. Generally, in DSC analyses of restrained oriented samples, the melting point is above that of the unoriented sample, and it increases with increasing degree of orientation and heating rate. In similar experiments with unrestrained samples the trends are more ambiguous: the melting point can be below or above that of the unoriented sample, and it may increase or decrease with increasing degree of orientation and heating rate.

The discussion above, coupled with the heating rate effects reported in the Results section, indicates that the fibers are unrestrained (i.e., free to shrink and reorganize) during our DSC measurements. Hence, the results obtained at the highest heating rate are closest to the true (hypothetical) values.

In a series of hot-stage microscopy experiments,⁸ fibers were placed between films made by quenching the same polymer and melted. The films melt at around 160°C. The fibers melt at higher temperatures, still being perfectly straight. For these experiments, in contrast to the DSC analyses, the melting point is positively correlated with the draw ratio. The fiber with draw ratio 3.5 in Figure 3 melts at around 190°C.

Melting Temperature Variations

Different definitions of the melting point are used in the literature; the onset of melting, the peak of the endotherm, and the temperature at which the last crystallite melts. The equilibrium melting point has a precise definition. However, most polymer samples are metastable and heterogeneous, and all the three definitions above characterize the sample. In this study, the onset of melting is found to be very sensitive to material and processing parameters. Most of the discussion below will deal with this value. The (first) peak of the endotherm shifts in the same way as the onset of melting, as in most other studies. The variations of the end of the melting regime will also be discussed.

The difference between the lowest and the highest value for the onset of melting, at a given heating rate, is more than 10°C. There are two major effects (draw ratio and polydispersity) and two minor effects (extrusion temperature and annealing ratio). These effects may be elucidated by considering fiber structure, structural (internal) restraints, and melting dynamics.

Shifts in the melting peaks for oriented polymer samples are often explained by the "oriented melt" concept or by crystallite sizes, as summarized in the next two paragraphs.

For an externally restrained deformed sample of a crosslinked polymer, the equilibrium melting point

increases with increasing tension and deformation, as expressed by the modified Clausius–Clapeyron equation, since the deformation is maintained during melting.⁷ Melting temperature vs. extension ratio for crosslinked systems has been modeled, assuming that the deformation only affects the amorphous phase (in both solid and melt at the melting point). (This is analogous to the argument used for explaining the high crystallization temperatures in oriented polymer melts: the entropy of fusion is low because the entropy of the oriented melt already is low.) With this approach, the increase in the equilibrium melting point can be written as a function of the extension ratio and the number of segments between network nodes, using rubber elasticity theory.⁹ Modifications of this expression, taking into account crystal size effects, have been used to explain the increase in melting point vs. degree of orientation for semicrystalline polymers without crosslinks, such as PET¹⁰ and PP.¹¹ The existence of temporary entanglement networks may justify the use of this approach on such polymer systems. This “oriented melt” concept has been refined in various ways through the years, but the theoretical basis is still unclear.⁷

The effect of crystal dimensions on the melting temperature is well known for unoriented polymer samples. Measurements of crystallite thickness have also been used to explain the melting temperature variations for PP fibers. Nurul Huda et al.¹² observed that the melting point and the crystallite thickness increased with increasing draw ratio. Furthermore, the melting point was found to be a linear function of the reciprocal crystallite thickness, in correspondence with the Thomson–Gibbs relation.⁷

Melting temperatures (and onset of melting values) that increases with increasing degree of orientation have been explained by the “oriented melt” concept or crystallite sizes, as outlined in the two paragraphs above. In our study, with unrestrained fibers, the onset of melting decreases with increasing draw ratio, while the end of the melting regime shifts to higher temperatures. WAXS results indicate that the order and/or size of crystallites decrease with increasing draw ratio. Furthermore, the microvoid volume fraction increases with increasing draw ratio, because the density decreases with increasing draw ratio, while the heat of fusion increases slightly. These effects could explain a decrease in the melting point, because the melting is initiated at defect sites on crystallite surfaces, the melting point decreases with decreasing crystallite size, and the melting rate increases with increasing chain mobility. However, these effects do not explain why the onset of melting

for restrained fibers increases with increasing draw ratio, as observed by hot-stage microscopy.⁸

Hence, we will modify the explanation given above, taking into account the effect of restraints. Our modified explanation is based on the relation between melting temperature, entropy of fusion, and enthalpy of fusion at equilibrium. We propose that for the crystallites that melt first, in fibers with high draw ratios, the change in enthalpy is lower or equal to that in fibers with lower draw ratios, due to defects and large surface areas. Furthermore, the change in entropy may be higher or equal to that in fibers with lower draw ratios, due to higher orientation in the solid state, less structural restraints, and more free volume for abrupt disorientation. These relations may explain why the onset of melting decreases with increasing draw ratio for fibers without external restraints.

For externally restrained fibers, the orientation may be transferred to the melt to a larger extent, and the “oriented melt” concept is valid. Hence, the onset of melting increases with increasing draw ratio.

The end of the melting regime is shifted to higher temperatures as the draw ratio increases. This could be explained by the “oriented melt” concept, because internal restraints are more likely to exist for the chains in the most oriented structural elements, such as fibril cores based on long chain nuclei. Such structures may also have a high intrinsic melting point, due to the long fold length (low enthalpy).

The second effect on the onset of melting to be discussed is that of the extrusion temperature. It must be noted that all other fiber properties are related to the extrusion temperature via the spinline stress. Furthermore, for the processing window in this study, the draw-down ratio has the largest effect on the spinline stress. Hence, the effect of extrusion temperature on the onset of melting is not related to the molecular orientation. Instead, a tentative explanation for this effect is that the number of entanglements transferred to the solid state increases with decreasing extrusion temperature.^{13–15} A higher entanglement density in intercrystalline domains may enhance the internal restraints.

The efficiency of the disentanglement in the spinline increases with increasing temperature and increasing stress. The crystallization temperature increases with increasing spinline stress,¹⁶ caused by either increasing the draw-down ratio or decreasing the extrusion temperature. Hence, only considering the temperature history, the degree of disentanglement should increase with increasing extrusion temperature. The stress at the exit of the

spinneret increases with decreasing extrusion temperature. However, the stress during solidification may depend less on the extrusion temperature. (The kinetics of the orientation-induced crystallization of a viscoelastic medium is complex, and not the topic of this article.) The structure elements with the lowest melting points probably belong to the a^* -oriented population,¹⁷ which crystallize at low stresses.² In conclusion, the entanglement density may be higher for a lower extrusion temperature. Qin et al.¹⁸ claim that the swelling DSC method is well suited for characterizing entanglements.

The lower onset of melting observed for narrow MWD fibers is probably due to less internal restraints, because the high molecular weight tail of the MWD is absent. At high draw-down ratios, the onset increases with increasing draw-down ratio. Again, structural restraints may be the explanation. Fibrillar structures formed at these high draw-down ratio mainly influence the end of the melting regime. The increase in onset of melting with increasing annealing ratio must be due to reorganization and perfection during annealing.

Multiple Peaks

The following explanations for multiple peaks and/or broadening of the melting regime for oriented PP samples can be found in the literature: (1) multimodal/broad distributions of morphological forms, crystallographic forms, crystallite sizes, or crystallite order;^{12,19–23} (2) melting, recrystallization, and remelting, as well as reorganization below the onset of melting;²⁴ and (3) melting and (exothermic) shrinkage taking place concomitantly.⁶ Of these three, the first one is the most common. Explanation (1) and (2) have also been used to explain multiple peaks for unoriented PP samples.

There are large variations among the thermograms in the articles referred to above. One reason for this is that “oriented PP” is an ambiguous term—the morphology is just as important as the degree of orientation. Wunderlich,⁷ for instance, defined three major types of deformation, which may produce different morphologies: deformation by drawing or rolling, crystallization from solution or melt under conditions of flow or extension, and crystallization during extension under pressure. The fibers in our study have experienced the two first types of deformation. In general, multiple peaks may have different explanations, depending on the material characteristics, the deformation types involved, and the experimental procedures for the DSC measurements. Supplementary information is

needed for the interpretation. Special techniques such as modulated DSC^{25,26} and swelling DSC¹⁸ may provide new insight into these matters.

The effects of material parameters, processing conditions, and heating rate on the position and magnitude of the secondary peak, observed for fibers with low draw ratios, suggest that this peak may be due to the melting of structures that have been reorganized/perfected during the heating scan. Narrow MWDs, high draw ratios and low draw-down ratios generally lead to low density and order, and probably higher chain mobility. (The high molecular weight tail has been “removed” for narrow MWDs. This should increase the mobility directly, as well as indirectly, because there will be less constraints formed in the orientation-induced crystallization process.) Hence, fibers with such characteristics should be more prone to reorganization. Furthermore, the degree of reorganization will increase with decreasing heating rate.

As the draw ratio increases, the melting regime broadens, especially towards lower temperatures, and several maxima emerge on the DSC curve. The first and last peak seem to correspond to the primary and secondary peak observed for fibers with low draw ratios. The curve segment between these peaks is more noisy and has lower reproducibility. This may be due to shrinkage effects.⁶

CONCLUSION

The variation of material parameters and processing conditions for the compact-spinning process are reflected in the DSC curves. The relative effects of these variations are as for other fiber properties, with some exceptions. The most notable exception is that the effect of the draw-down ratio on the position of the first melting peak is small compared to that of the extrusion temperature.

A metastable heterogeneous system is probed when a polymer fiber is heated in a DSC instrument, and this complicates the interpretation of the endotherm. The thermal behavior is also affected by the state of the intercrystalline domains. With the sample preparation method used in this study, structural reorganization seems to occur during heating.

This article is based on results from the “Expomat Fiber Project,” supported by Borealis and the Research Council of Norway. The authors would like to thank T.-L. Rolfsen for carrying out some of the DSC measurements, and O. Hånde for helpful comments.

REFERENCES

1. E. Andreassen and O. J. Myhre, *J. Appl. Polym. Sci.*, **50**, 1715 (1993).
2. E. Andreassen, O. J. Myhre, E. L. Hinrichsen, and K. Grøstad, *J. Appl. Polym. Sci.*, **52**, 1505 (1994).
3. E. Andreassen, E. L. Hinrichsen, K. Grøstad, O. J. Myhre, and M. D. Braathen, *Polymer*, **36**, 1189 (1995).
4. M. Ahmed, *Polypropylene Fibers—Science and Technology*, Elsevier, Amsterdam, 1982.
5. M. Todoki, *Thermochim. Acta*, **93**, 147 (1985).
6. D. C. Sun and J. H. Magill, *Polym. Eng. Sci.*, **29**, 1503 (1989).
7. B. Wunderlich, *Macromolecular Physics, Vol. 3. Crystal Melting*, Academic Press, New York, 1980.
8. O. Hånde, to appear.
9. W. R. Krigbaum and R.-J. Roe, *J. Polym. Sci., Part A*, **2**, 4391 (1964).
10. P. Nicholas, A. R. Lane, T. J. Carter, and J. N. Hay, *Polymer*, **29**, 894 (1988).
11. A. O. Ibadon, *J. Appl. Polym. Sci.*, **43**, 567 (1991).
12. M. Nurul Huda, H. Dragaun, S. Bauer, H. Muschik, and P. Skalicky, *Colloid Polym. Sci.*, **263**, 730 (1985).
13. R. K. Bayer, *Colloid Polym. Sci.*, **269**, 421 (1991).
14. R. K. Bayer, F. Liebentraut, and T. Meyer, *Colloid Polym. Sci.*, **270**, 331 (1992).
15. R. K. Bayer, *Colloid Polym. Sci.*, **272**, 910 (1994).
16. F.-M. Lu and J. E. Spruiell, *J. Appl. Polym. Sci.*, **34**, 1541 (1987).
17. K. Katayama, T. Amano, and K. Nakamura, *Kolloid-Z. Z. Polym.*, **226**, 125 (1968).
18. J. Qin, P. Hu, J. Zhao, Z. Wu, and B. Qian, *J. Appl. Polym. Sci.*, **51**, 1433 (1994).
19. H. Tanaka, N. Takagi, and S. Okajima, *J. Polym. Sci., Polym. Chem. Ed.*, **12**, 2721 (1974).
20. R. J. Samuels, *J. Polym. Sci., Polym. Phys. Ed.*, **13**, 1417 (1975).
21. S. J. Pan, H. I. Tang, A. Hiltner, and E. Baer, *Polym. Eng. Sci.*, **27**, 869 (1987).
22. A. K. Taraiya, A. P. Unwin, and I. M. Ward, *J. Polym. Sci., Polym. Phys. Ed.*, **26**, 817 (1988).
23. R. J. Yan and B. Jiang, *J. Polym. Sci., Polym. Phys. Ed.*, **31**, 1089 (1993).
24. Y. Maeda, K. Nakayama, and H. Kanetsuna, *Polym. J.*, **14**, 295 (1982).
25. M. Reading, A. Luget, and R. Wilson, *Thermochim. Acta*, **238**, 295 (1994).
26. B. Wunderlich, Y. Jin, and A. Boller, *Thermochim. Acta*, **238**, 277 (1994).

Received January 8, 1995

Accepted March 3, 1995